

## EFFECT OF HEATING RATES IN NATURAL FIRES ON THE THERMAL PERFORMANCE OF A SOLVENT-BORNE INTUMESCENT COATING



Peter Schaumann<sup>1</sup>



Waldemar Weisheim<sup>2</sup>

### ABSTRACT

The aim of this paper is to study the thermal performance of an industrially manufactured solvent-borne intumescent coating in case of natural fires. The intumescent coating is originally designed to protect steel members in case of ISO-standard fire. In the first part of the study the thermal performance of the coating is evaluated for various heating rates using thermogravimetric analyses. It is demonstrated that the mass loss of the coating shows a clear dependency on the heating rate during the reaction step of intumescence. In the second part of the study the thermal insulation efficiency of the coating is investigated using small scale furnace tests with an innovative test setup. The tests show distinctively that the best fire protective performance is achieved for high heating rates.

### 1 INTRODUCTION

In Europe the insulating efficiency of intumescent coatings (ICs) is verified by small scale fire tests according to ETAG 018 part 2 [1]. Within these fire tests coated steel plates are exposed to ISO-standard fire. Therefore, the assessment of the thermal performance of intumescent coatings is solely related to this fire scenario. Since harmonised rules for the design of structural steel members have been introduced in Europe in 2012, steel structures with intumescent coatings can also be designed under the assumption of natural fire scenarios. Therefore, it is of great importance to investigate the thermal performance of intumescent coatings when being exposed to heating rates deviating from ISO-standard fire conditions.

In this study, the efficiency of an industrially manufactured solvent-borne intumescent fire protective coating is investigated using laboratory tests (analysis of thermal stability characteristics) as well as small scale furnace tests (measurement of the temperature profile on the backside of a coated steel plate and inside the formed char when exposed to various constant heating rates).

---

<sup>1</sup> Full Professor. Institute for Steel Construction, Leibniz Universität Hannover. GERMANY. e-mail: schaumann@stahl.uni-hannover.de.

<sup>2</sup> PhD Student. Institute for Steel Construction, Leibniz Universität Hannover. GERMANY. e-mail: weisheim@stahl.uni-hannover.de. **Corresponding Author.**

## 2 EXPERIMENTAL

### 2.1 Material and sample preparation

A commercially available solvent-borne intumescent coating is used in this study. The coating is based on a solvent binder into which fire retardant agents such as ammonium polyphosphate (APP) and pentaerythritol (PER) are incorporated. The intumescence reaction is ensured through the blowing agent melamine (MEL).

Table 1. Dry film thickness (DFT) and heating rates of the performed fire tests

Sample ID (-)	Heating rate (°C/min)	Configuration (-)	DFT (µm)
H10	10	A	-
H10S-1	10	A	460
H10S-2	10	B	410
H10S-3	10	B	475
H30	30	A	-
H30S-1	30	A	475
H30S-2	30	B	475
H30S-3	30	B	470
H50	50	A	-
H50S-1	50	A	410
H50S-2	50	B	420
H50S-3	50	B	460

For the thermogravimetric analyses the coating has been applied on a glass plate and was tried at room temperature and normal humidity for five weeks. Subsequently, the coating was removed from the glass plate and was processed into a fine, white powder.

For the small scale furnace tests the coating was applied at a desired dry film thickness (DFT) of 400 µm on steel plates with dimensions of 90 x 100 x 5 mm (see Fig. 1). First, the viscous coating was applied via scaper on the prepared steel plates. Then, the surface of the coating was levelled and smoothed thus resulting in an even layer. Subsequently, the coating was dried at room temperature and normal humidity for five weeks. The DFT of each specimen was measured equidistantly at 30 points using an analogue thickness gauge (Mikrotest IV, ElektroPhysik). The averaged DFTs are listed in Table 1.

### 2.2 Thermogravimetric (TG) analysis

The TG analyses of the solvent-borne intumescent coating were carried out at 10, 30 and 50 °C/min under synthetic air (80 % Ar and 20 % O<sub>2</sub>), using a NETZSCH STA 409 PC/PG DSC-TGA analyser. The samples (approximately 8 mg, in powder form) were placed in closed aluminium oxide (Al<sub>2</sub>O<sub>3</sub>) pans. The precision of the weight measurement was 20/30000 mg over the whole range of temperature (40 - 600 °C). The error of temperature measurement was ± 1 °C.

### 2.3 Fire protection test

The small scale furnace tests were performed to evaluate the thermal insulation efficiency of the solvent-borne intumescent coating at constant heating rates of 10, 30 and 50 °C/min (at first without the investigation of the cooling branch). Therefore, three different types of specimens were chosen. The first type of specimens was an uncoated steel plate (H10, H30 and H50) which serves as a reference (see Table 1). The second type of specimens was a coated steel plate (H10S-1, H30S-1 and H50S-1). For both, unprotected and protected specimens the steel temperature was measured using K-type thermocouples with a diameter of 0.51 mm applied on the backside of the steel plate. This way of temperature measurement is denoted in this paper as 'configuration A'. Additionally, a

third type of specimens (H10S-2/3, H30S-2/3 and H50S-2/3) was investigated using the innovative test setup shown in *Fig. 1*. The innovation of this test setup is characterised by the configuration of the K-type thermocouples ensuring both the measurement of the steel plate and the char temperature at different heights (0, 3, 6, 9 and 12 mm) due to a one-dimensional heat flux. For this test setup five holes with a diameter of 2.5 mm were drilled into the steel plate before the coating was applied (see *Fig. 1*). Then, the thermocouples were inserted through the drilled holes and the test specimen was embedded horizontally in a vermiculite plate ensuring adiabatic conditions. This type of temperature measurement is denoted in this paper as 'configuration B' (see *Table 1*).

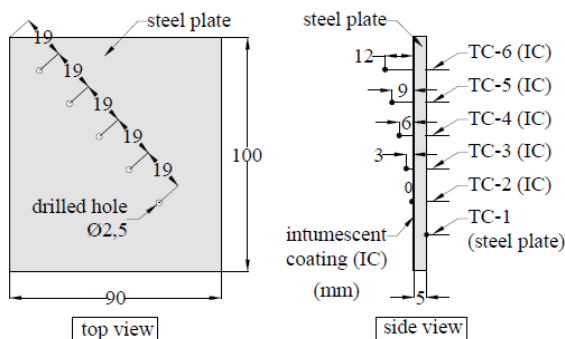


*Fig. 1.* Dimension of the test specimen (left) and configuration of thermocouples for the measurement of char and steel plate temperatures (right)

A total number of nine coated and three uncoated test specimens were prepared for the small scale furnace tests. The tests were performed using an electric furnace with a volume of 1000 cm<sup>3</sup> (Naberthern LE 1/11). The steel plate, char and furnace temperatures were measured every 0.5 s using a QuantumX MX1609KB (HBM GmbH) with an error of  $\pm 1$  °C over the whole range of temperature (20 – 1000 °C).

### 3 RESULTS AND DISCUSSION

#### 3.1 Thermal degradation

The thermogravimetric (TG) analyses were used to investigate the thermal stability and degradation behaviour of the solvent-borne intumescent coating at different heating rates. The TG and DTG curves of the investigated samples are shown in *Fig. 2*. The thermal stability characteristics are presented in *Table 2*.

The thermal degradation of the solvent-borne intumescent coating occurs in three main steps within the investigated range of temperature (40 – 600 °C). At the heating rate of 10 °C/min the first step of thermal degradation arises between 40 and 252 °C and results in a residual weight of 96.5 %. With increasing heating rates the end of the first step of degradation shifts into higher temperatures, thus resulting in higher initiation temperatures for the second step of degradation, e.g. 268 °C for the heating rate of 30 °C/min. At the end of the first step the residual weight of all samples is nearly the same (10 °C/min: 96.5 %, 30 °C/min: 96.9 % and 50 °C/min: 96.6 %) as it can be seen from the thermal stability characteristics in *Table 2*. The mechanism of thermal degradation of intumescent fire protective coatings has been studied by many different authors, i.a. by Branca et al. [2]. According to Duquesne et al. [3] the mass loss of intumescent coatings within the first step is characterized by the thermal degradation of the binder.

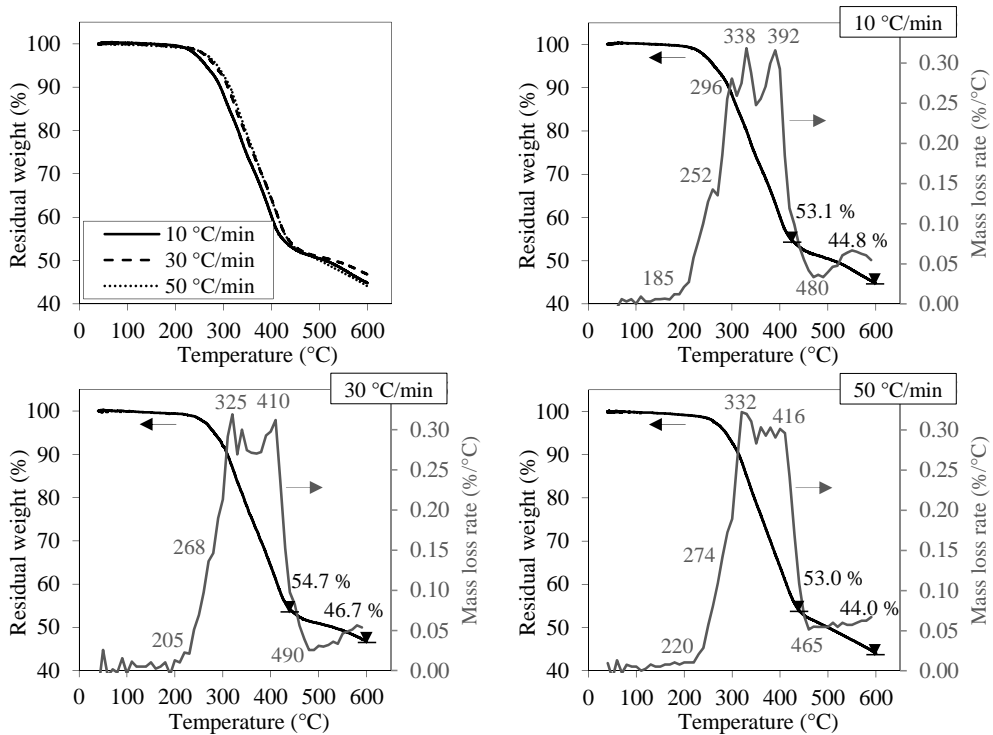


Fig. 2. TG and DTG curves of the solvent-borne IC at heating rates of 10, 30 and 50 °C/min

With further increase in temperature the second step of thermal degradation occurs, leading to the highest change in mass loss (see DTG curves in Fig. 2). For 10 °C/min the second step of thermal degradation arises between 252 and 422 °C and leads to a residual weight of 53.1 %. In correspondence with the thermal behaviour of the coating in the first step, a shift in temperature is noticeable also in the second step of degradation with increasing heating rates, e.g. 448 °C for the heating rate of 50 °C/min. Nevertheless, the temperature spread (228 – 237 °C) of the second degradation step remains for all heating rates almost equal. Consequently, at the end of the second step the temperature increases with increasing heating rates (see Table 2). The residual weight at the end of the second step is for 10 and 50 °C/min nearly the same (53.1 % compared to 53.0 %). Only the sample with 30 °C/min shows at the end of the second step (436 °C) a residual weight of 54.7 % and thus a marginally higher thermal stability. Although the second step of thermal degradation underlies a temperature shift, the residual weight of all samples is nearly the same for 500 °C (10 °C/min: 50.5 %, 30 °C/min: 50.9 % and 50 °C/min: 50.0 %) as it can be seen from the TG curves in Fig. 2. According to Wang et al. [4] the mass loss between 220 and 420 °C is characterized in principal by the thermal degradation of the blowing agent within the fire protective coating. Since melamine (MEL) is often used as blowing agent for intumescent coatings, the thermal degradation of the heterocyclic tri-amino compound has been investigated by Ledeti et al. [5] and Derakhshesh et al. [6] at different heating rates. For both, oxygen and air atmosphere melamine shows a degradation shift with increasing heating rates. From 10 to 20 °C/min the degradation step shifts from approximately 220 – 370 °C to 280 – 400 °C. With further increase in temperature the residual mass of MEL remains unchanged. Taking this as a basis leads to the assumption that the observed crucial mass loss of the solvent-borne intumescent coating is directly related to the thermal stability characteristics of MEL. Therefore, the phenomenon of degradation

shift of the investigated intumescent coating with increasing heating rates can be explained by the thermal stability characteristics of MEL referring to Ledeti et al. [5] and Derakhshesh et al. [6]. Similar knowledge has been gained by Jimenez et al. [7] when analysing the reaction kinetics and thermal degradation of an epoxy-based intumescent coating under various heating rates. The third step of thermal degradation is characterized by a lower mass loss (about 0.05 %/°C, see Fig. 2) compared to the second step. During this phase no significant difference in degradation behaviour is identifiable for heating rates of 10 and 50 °C/min (44.8 % compared to 44.0 %). Since the mass loss rate is unequal to zero for all investigated heating rates, the degradation process is still in process at 600 °C. Therefore, a further decrease in residual weight is expected with increasing temperatures.

Table 2. Thermal stability characteristics of the investigated solvent-borne IC. Error  $\pm 1$  °C and  $\pm 0.02$  weight %

Heating rate (°C/min)	T <sub>(2%)</sub> (°C)	T <sub>max</sub> 1 <sup>st</sup> step (°C)	Mass 1 <sup>st</sup> step (%)	T <sub>max</sub> 2 <sup>nd</sup> step (°C)	Mass 2 <sup>nd</sup> step (%)	T <sub>max</sub> 3 <sup>rd</sup> step (°C)	Mass 3 <sup>rd</sup> step (%)	Mass T <sub>500°C</sub> (%)
10	237	252	96.5	422	53.1	600	44.8	50.5
30	254	268	96.9	436	54.7	600	46.7	50.9
50	257	274	96.6	448	53.0	600	44.0	50.0

### 3.2 Fire protection of the coating

The temperature-time curves of the performed small scale furnace tests are shown in Fig. 3. The essential corresponding thermal characteristics are summarised in Table 3.

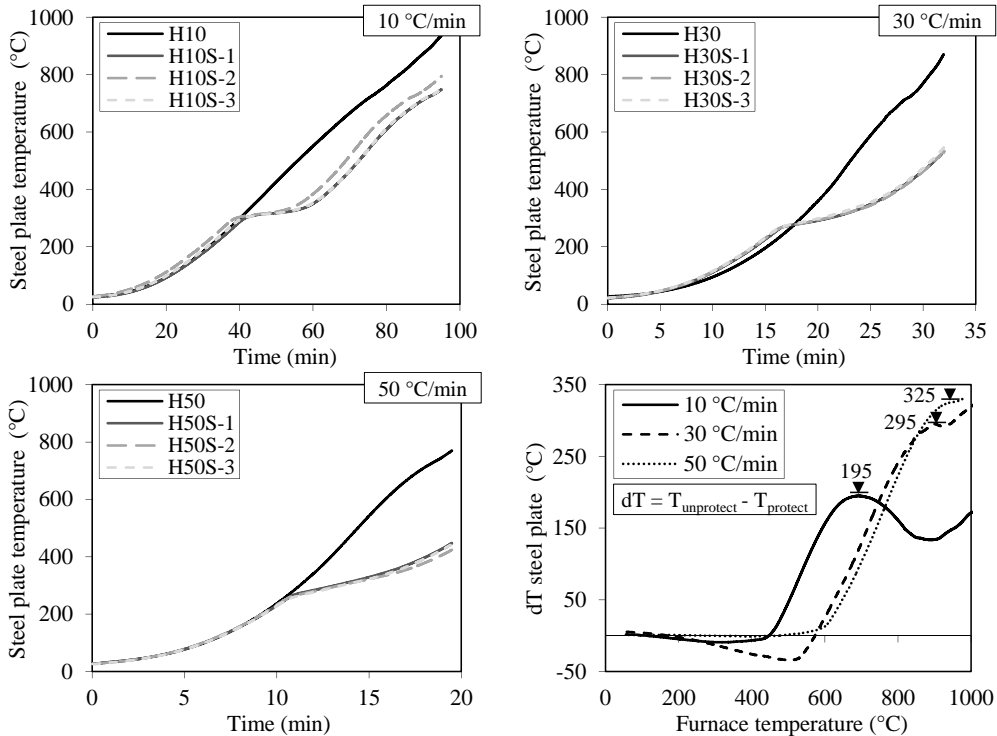
In the diagrams of Fig. 3 for each investigated heating rate (10, 30 and 50 °C/min) temperature-time curves of three coated (configuration A and B) and one uncoated steel plate (configuration A) are given. Since the measured temperature profiles of the coated samples follow the same trend respectively for each heating rate, it is evident that the application of thermocouples within the intumescent char (configuration B) does not influence the temperature results noticeably. Thus, a high reproducibility for the performed furnace tests is given.

Table 3. Averaged steel temperatures (T<sub>max</sub>) and difference in temperature (dT<sub>max</sub>) between unprotected and protected steel plates due to heating rates of 10, 30 and 50 °C/min

Heating rate (°C/min)	T <sub>max</sub> 1 <sup>st</sup> step (°C)	T <sub>furnace</sub> 1 <sup>st</sup> step (°C)	T <sub>max</sub> 2 <sup>nd</sup> step (°C)	T <sub>max</sub> 3 <sup>rd</sup> step (°C)	dT <sub>max</sub> (°C)	T <sub>furnace</sub> at dT <sub>max</sub> (°C)
10	298	455	365	668	195	680
30	266	532	349	-	295	897
50	260	605	334	-	325	943

For both, protected and unprotected samples the temperature-time curves for each heating rate follow the same progression during the first step. This is particularly noticeable for 50 °C/min (see Fig. 3). The point in time or temperature at which the temperature-time curves of the coated and uncoated samples begin to deviate corresponds to the beginning of the reaction and intumescence process of the coating. The differences in temperature (dT) between the unprotected and the protected steel plates are given for all three heating rates by differential curves as a function of the furnace temperature in Fig. 3. With increasing heating rates the beginning of the intumescence reaction occurs at higher furnace temperatures (10 °C/min: 455 °C, 30 °C/min: 532 °C, 50 °C/min: 605 °C). Nevertheless, during this step the highest steel temperature arises for the lowest heating rate (298 °C) as it can be seen in Table 3. The reason for this contrary behaviour can be described by thermal inertia of the steel plates. This effect is especially quantifiable for the unprotected steel plates (see Fig. 4). As it can be seen higher furnace temperatures are needed to achieve the same steel temperature when the heating rates are increased. The effect of thermal inertia is eliminated in

the dT-curves of *Fig. 3*. Therefore, the differences in furnace temperature for increasing heating rates are solely characterised by the thermal protection of the coating. Taking the dT-curves as a basis, the best thermal protection of the coating occurs for the highest heating rate. Whilst the difference in temperature between the unprotected and protected steel plates is 195 °C for 10 °C/min, the heating rate of 50 °C/min results in a temperature difference of 325 °C. The fact that the point of maximum temperature difference shifts with increasing heating rates into higher temperatures (10 °C/min: 680 °C, 30 °C/min: 897 °C, 50 °C/min: 943 °C, see *Table 3*) is affiliated to the thermal characteristic of the investigated coating. This phenomenon has already been observed within the thermogravimetric analyses.



*Fig. 3.* Comparison between steel temperatures of protected and unprotected steel plates due to heating rates of 10, 30 and 50 °C/min

The thermal insulation efficiency of the investigated intumescent fire protective coating can be assessed very well by the derivative steel temperatures in *Fig. 4*. For all heating rates a significant reduction in speed of warming occurs when the coating starts to form the heat-insulating char resulting in a minimum at 319, 276 and 273 °C for 10, 30 and 50 °C/min. The period at which the speed of warming decrease and increase again is more pronounced for higher heating rates than for lower one. Therefore, again the best thermal protection of the investigated coating can be observed for the highest heating rate.

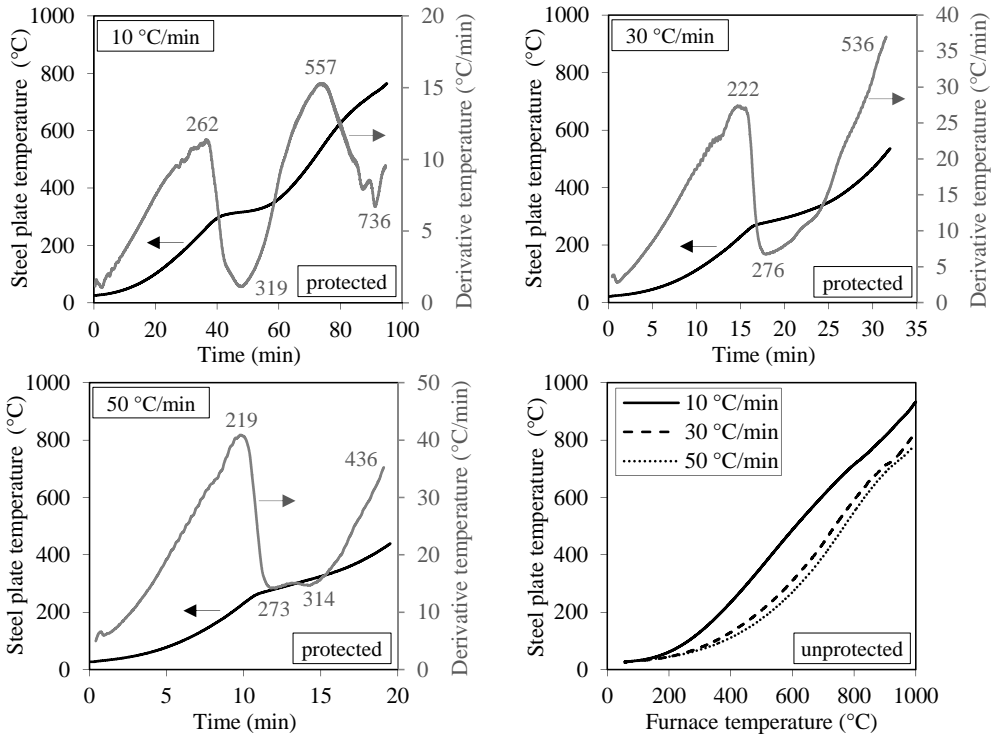


Fig. 4. Steel temperatures of protected (averaged) and unprotected steel plates and their derivative due to heating rates of 10, 30 and 50 °C/min

### 3.3 Thermal behaviour of the intumescent char

In addition to the measured steel plate temperatures the thermal insulation efficiency of the investigated coating can be evaluated by the measured char temperatures. Due to limitations of space no temperature-time curves of the thermocouples TC-2 to TC-6 positioned inside the char (see Fig. 5) are shown in this paper. Instead, the measured temperature profiles within the formed intumescent char are shown exemplarily for 10 and 50 °C/min at different point in time in Fig. 6.

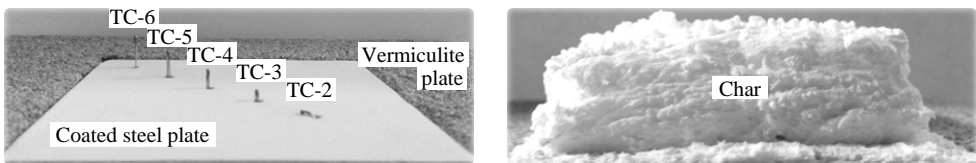


Fig. 5. Coated steel plate with applied thermocouples (left) and formed intumescent char after fire exposure (right).

During the phase of maximum thermal insulation efficiency (see Fig. 4) a nonlinear temperature gradient occurs inside the intumescent char for both 10 and 50 °C/min. Due to the differences in reaction time resulting from various heating rates, the nonlinear temperature gradient is more significant for the higher heating rate. Since a higher thermal insulation efficiency was observed for higher heating rates, the thermal insulation efficiency of the coating is directly related, amongst others, to the temperature profile inside the formed char. In addition to the observed nonlinear temperature gradient, also linear temperature gradients occur inside the char before and after the phase of maximum thermal protection. Due to the difference in reaction time this phenomenon appears only for 10 °C/min.

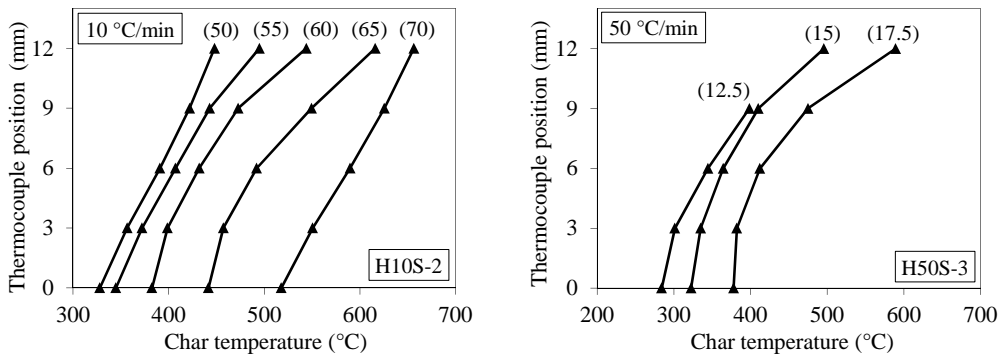


Fig. 6. Measured temperature profile inside the intumescent char for 10 and 50 °C/min at different points in time (min)

#### 4 CONCLUSIONS

The aim of this paper was to study the thermal stability characteristics and insulation efficiency of a commercially available solvent-borne intumescent coating in case of natural fires.

Thermogravimetric analyses for various heating rates show a clear inversely proportional dependency between the thermal degradation of the coating and the increase in heating rates during the reaction step of intumescence. The observed shift in temperature is assumed to be related to the thermal behaviour of MEL. In addition, small scale furnace tests, using an innovative test setup, show distinctively that the best fire protective performance of the investigated coating is achieved for the highest investigated heating rate. The thermal insulation efficiency is directly related to the measured nonlinear temperature profile inside the formed char. Taking this as a basis it is of great importance to consider the heating rate dependent thermal performance of intumescent coatings when the heating behaviour of coated steel structures is evaluated or numerical simulations (e.g. Schaumann et al. [8]) are performed.

#### REFERENCES

- [1] European Organization for Technical Approvals (2006). *ETAG 018, Guideline for European Technical Approval of fire protective products, Part 2: Reactive coatings for fire protection of steel elements* (2006).
- [2] Branca C., Di Blasi C. (2002). *Analysis of the Combustion Kinetics and Thermal Behavior of an Intumescent Coating*. Ind. Eng. Chem. Res. 41 (2002), pp. 2107–2114.
- [3] Duquesne S, Magnet S., Jama C., Delobel R. (2004). *Intumescent paints: fire protective coatings for metallic substrates*. Surface and Coatings Technology 180-181 (2004), pp. 302–307.
- [4] Wang G., Yang, J. (2011). *Thermal degradation study of fire resistive coatings containing melamine polyphosphate and dipentaerythritol*. Progress in Organic Coatings 72 (2011), pp. 605–611.
- [5] Ledeti I., Vlase G., Vlase T., Doca N., Bercean V., Fulias A. (2014). *Thermal decomposition, kinetic study and evolved gas analysis of 1,3,5-triazine-2,4,6-triamine*. J Therm Anal Calorim 118 (2014), pp. 1057–1063.
- [6] Derakhshesh Z., Khorasani M., Akhlaghi S., Keyvani B., Alvani A. (2012). *Design and optimization of an intumescent flame retardant coating using thermal degradation kinetics and Taguchi's experimental design*. Polym Int 61 (2012), pp. 926–933.
- [7] Jimenez M., Duquesne S, Bourbigot S. (2009). *Kinetic analysis of the thermal degradation of an epoxy-based intumescent coating*. Polymer Degradation and Stability 94 (2009), pp. 404–409.
- [8] Schaumann P., Tabelaing F., Weisheim W.: *Numerical simulation of the heating behaviour of steel profiles with intumescent coating adjacent to trapezoidal steel sheets in fire*, Journal of Structural Fire Engineering 7 (2) (2016), pp. 158-167.